Microfluidics and Nanofluidics (2018) 22:19
https://doi.org/10.1007/s10404-018-2034-8

RESEARCH PAPER

Liquid and gas flows in microchannels of varying cross section: a comparative analysis of the flow dynamics and design perspectives

Vadiraj Hemadri[1] · V. S. Duryodhan[1] · Amit Agrawal[1]

Received: 9 August 2017 / Accepted: 9 January 2018 / Published online: 24 January 2018

Abstract

This paper presents a comparative study of the flow of liquid and gases in microchannels of converging and diverging cross sections. Towards this, the static pressure across the microchannels is measured for different flow rates of the two fluids. The study includes both experimental and numerical investigations, thus providing several useful insights into the local information of flow parameters as well. Three different microchannels of varying angles of convergence/divergence (4°, 8° and 12°) are studied to understand the effect of the angle on flow properties such as pressure drop, Poiseuille number and diodicity. A comparison of the forces involved in liquid and gas flows shows their relative significance and effect on the flow structure. A diodic effect corresponds to a difference in the flow resistance in a microchannel of varying cross section, when the flow is subjected alternatively to converging and diverging orientations. In the present experiments, the diodic effect is observed for both liquid and gas as working fluids. The effect of governing parameters—Reynolds number and Knudsen number, on the diodicity is analysed. Based on these results, a comparison of design perspectives that may be useful in the design of converging/diverging microchannels for liquid and gas flows is provided.

1 Introduction

Diverging and converging microchannels are an important part of microdevices. Flow in such geometries is implicit to the design of devices like converging–diverging micronozzles, valveless micropumps and micromixers (Stemme and Stemme 1993; Lauga et al. 2004; Akbari et al. 2010). They are also likely to be employed in microchannels for reducing two-phase flow instability (Agrawal et al. 2012). MEMS devices, due to their compact nature, often have space constraints and may include sections like converging and diverging channels or sudden expansion and contraction in their design. Microchannels of gradually varying cross section have also been applied for heat transfer augmentation, accelerated particle electrophoresis and polymer processing (Akbari et al. 2011). These applications require a fundamental knowledge of fluid flow in varying cross section microchannels, and from a designer's perspective, experimental data can provide some empirical correlations acting as pointers to the design of such devices. Currently, the data available for microflow in such geometries are rather limited and the present study should be helpful in this regard by bringing out the flow physics in terms of pressure drop, velocity distribution and flow structure.

Stemme and Stemme (1993) experimentally studied the flow in diffuser and nozzle elements for their application in valveless micropumps. This idea was further investigated in detail by several other studies (Olsson et al. 1996, 2000; Singhal et al. 2004). These studies explored the effect of Reynolds number on the flow rectification property of the micropumps and found that the rectification properties improved for high Reynolds numbers. Gerlach (1998) followed an empiro-theoretical approach to study the flow behaviour in microdiffusers in the context of dynamic passive valves in micropumps. The flow rectification efficiency was identified to be a function of aperture angle, relative microchannel length, throat rounding and flow velocity. Akbari et al. (2010) developed an analytical model to predict the frictional flow resistance in periodically converging–diverging microtubes for laminar flow conditions. They found the flow resistance to be independent of the Reynolds number but depending only on the geometrical parameters. Akbari et al. (2011) proposed an approximate method for determining the pressure drop in laminar, single phase flow in microchannels of slowly varying cross sections of

✉ Amit Agrawal
amit.agrawal@iitb.ac.in

[1] Department of Mechanical Engineering, Indian Institute of Technology Bombay, Powai, Mumbai 400076, India

arbitrary shapes. They proposed a non-dimensional number that could serve to compare the relative significance of viscous and inertial effects under such flow conditions. Tanaka et al. (2013) studied the effect of channel geometry on the pump head of a valveless micropump with diffuser–nozzle elements. He et al. (2017) studied the effect of diverging angle, volume flow rate and excitation frequency on the performance of converging/diverging elements in a piezoelectric passive micropump. They found that diverging flow dominated the flow-directing capability of the micropump for a range of divergence angles ($10° < \theta < 20°$). Beyond these limits, the flow was seen to be independent of the diverging angle and converging mode dictated the pump performance.

The above studies pertain to liquid flow in diverging/converging microchannels. In case of gas flow in microchannels of non-uniform cross sections, Sharipov and Bertoldo (2005) proposed a method to predict the mass flow rate of rarefied gas flow in a long tube of variable radius. Graur et al. (2014) compared the flow of gas in varying cross section microchannels in converging and diverging orientations. They reported that the diodicity is a function of rarefaction and exists only in the slip flow and transition flow regimes. Graur et al. (2016) studied the diodic effect in gaseous flows in various types of microchannels. In particular, they studied the effect of having the height or width as the varying dimension along the length of the microchannel. Szalmas et al. (2015) showed that the diodic effect is absent for gas flows in the continuum regime and the free molecular regime and has a maximum value in the slip/transition regime.

Flow in diverging and converging microchannels has been studied for water flow under isothermal conditions by Duryodhan et al. (2012, 2014), respectively. They proposed an approach to determine an 'equivalent hydraulic diameter', which is the hydraulic diameter obtained at a particular location of varying cross section microchannel, which gives the same pressure drop as that of a constant cross section microchannel under otherwise same flow conditions. Varade et al. (2015a, b) adopted a similar approach to obtain the equivalent hydraulic diameter for diverging and converging microchannels for gas flows using nitrogen as the fluid. Hemadri et al. (2016, 2017) extended the experiments on converging/diverging microchannels to cover the entire slip regime and early transition regime ($Kn \sim 2$). They provided the first experimental evidence of the existence of Knudsen minimum in microchannels of non-uniform cross sections. Study of gas flows through microchannels is different with respect to liquid flows due to the presence of additional effects, such as compressibility and rarefaction, that appear only in the case of gases. From the literature, it is observed that there have been independent studies relating the pumping ability of a micropump for liquid or gas flows using diffuser–nozzle elements. A comparison of flow in converging/diverging geometries with liquid and gas as working fluid has, however, not been carried out. Such a comparison is expected to explore the possibility of utilizing a micropump that can transfer both liquid and gas. A comparative analysis is also expected to bring out the effect of Reynolds number and Knudsen number on the pumping action and the conditions for optimum pumping efficiency for both liquid and gas flows.

This article aims to present a detailed and consolidated comparison of liquid and gas flow in converging and diverging microchannels by comparing the experimental data obtained by using deionized water and nitrogen as working fluids, respectively. The other aim is to highlight the changes in the flow structure and the relative significance of the forces involved (inertial, pressure and viscous force) for the case of liquid and gas flows. The effect of Reynolds number and Knudsen number on the flow diodicity is studied to understand the effect of these parameters on the pumping efficiency of a diffuser–nozzle micropump.

2 Experimental set-up and test sections

Figure 1a, b shows the schematic of the experimental arrangement to study the pressure drop in converging and diverging microchannels in the case of liquid and gas flows, respectively. In both the cases, a mass flow controller directs the fluid through the microchannel and the corresponding inlet and outlet pressure measurements are taken across the microchannel. Further details about the experimental arrangement for water and nitrogen flows can be found in Duryodhan et al. (2012) and Varade et al. (2015a), respectively.

The microchannels used in the experiments were fabricated in-house on a single-side polished, p-type silicon wafer of ⟨100⟩ orientation. The microchannels are fabricated using the conventional photolithography technique and wet etching the wafer using TMAH solution. This results in microchannels of trapezoidal cross section. The top of the microchannel is covered with an optically smooth quartz plate (Singh et al. 2008). Three different microchannels of different convergence/divergence angles are employed in this work. The schematic of the microchannel along with the converging/diverging orientation is shown in Fig. 2. The relevant dimensions along with the uncertainties are tabulated in Table 1. Note that the same set of microchannels is utilized for both liquid and gas flow measurements allowing for the direct comparison of the two cases.

Numerical simulations are carried out using commercial software (ANSYS Fluent). Figure 3 shows the geometry of the model employed in the simulations and the relevant boundary conditions. The computational domain is discretized by quadrilateral face elements and hexahedral volume

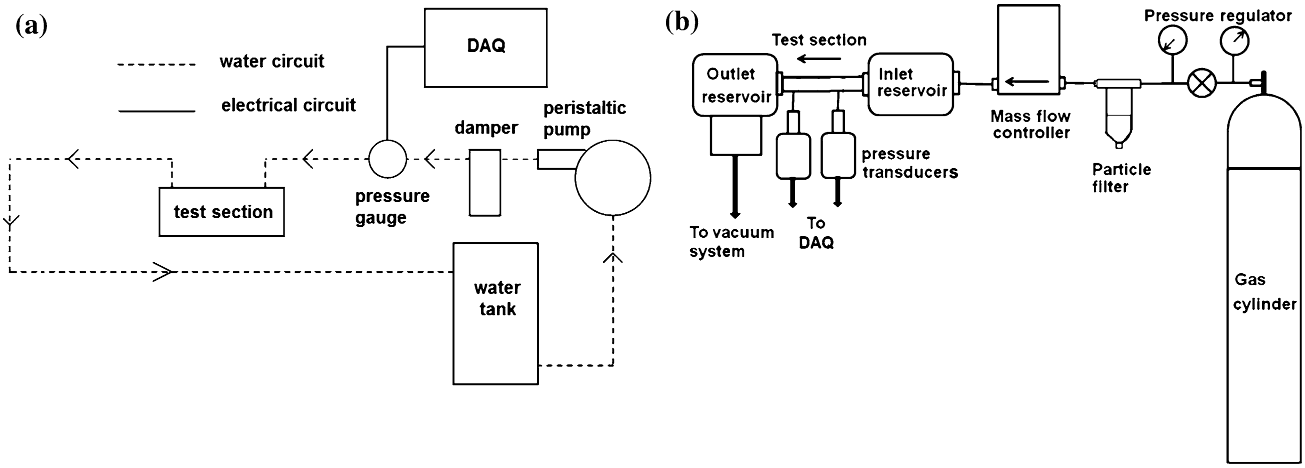

Fig. 1 Schematic of experimental arrangement for the case of **a** water, **b** nitrogen

Fig. 2 Schematic of the cross section and geometry of the microchannel

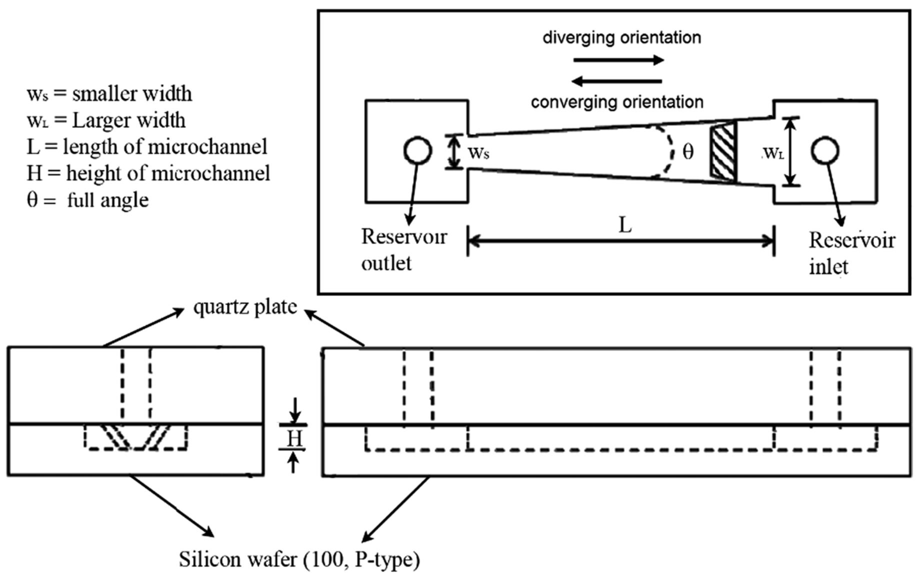

Table 1 Dimensional details of the microchannels employed in the experiments

Section	I	II	III	Uncertainty	Units
Smaller width (w_s)	213	211	211	± 2	μm
Bigger width (w_L)	1600	2997	4400	± 2	μm
Length (L)	20	20	20	± 0.1	mm
Height (H)	79	78	78	± 1	μm
Diverging/converging angle (θ)	4	8	12	0.5	degrees
Hydraulic diameter (D_h)	142	147	150	1.33	%

elements. The Navier–Stokes equations are solved with finite volume discretization for the case of both liquid and gas flows. A pressure-based solver is utilized with SIMPLE algorithm for pressure–velocity coupling. The main distinction between the simulations for water and nitrogen flow is the modification of the wall boundary condition: from no slip used for water flow to low-pressure boundary slip module, in the case of nitrogen flow. More details of the numerical model and the results of the grid independence test for liquid and gas flows can be found in Duryodhan et al. (2012) and Varade et al. (2015a), respectively.

3 Data reduction

From the measurement of mass flow rate and the corresponding pressures across the microchannel, various non-dimensional parameters are obtained to facilitate comparison between liquid and gas flows. All the parameters are obtained

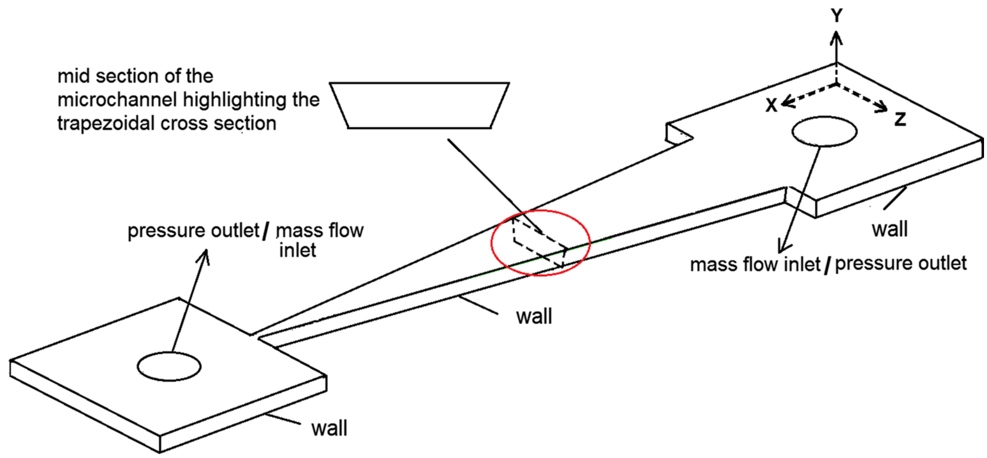

Fig. 3 Geometry of the simulated model along with the boundary conditions. The inlet and outlet boundary conditions are interchanged to study the flow in both converging and diverging orientations

using the mean hydraulic diameter (D_h) calculated at the mid-length of the microchannel. The Reynolds number (Re) is calculated as

$$Re = \frac{\dot{m} D_h}{\mu A} \quad (1)$$

where $\dot{m}$ is the mass flow rate, μ is the dynamic viscosity, and A is the cross-sectional area at the mid-length of the microchannel. For liquid flows, the Darcy friction factor is obtained as

$$f = \left(\frac{D_h}{L}\right)\frac{\Delta P}{2\rho u^2} = \left(\frac{D_h}{L}\right)\left(\frac{\Delta P \rho}{J^2}\right) \quad (2)$$

where ΔP is the pressure drop across the microchannel, ρ is the density, J is the mass flux ($J = \dot{m}/A$), and L is the length of the microchannel. For the case of gas flows, an additional pressure drop is encountered due to the acceleration of the fluid. Hence, the Darcy friction factor for gases is defined as

$$f = \left(\frac{D_h}{L}\right)\left[\frac{1}{J^2 RT} - \frac{1}{P_i P_o}\right](P_i^2 - P_o^2) \quad (3)$$

where R is the specific gas constant, T is the absolute temperature, and P_i and P_o are the pressures at the inlet and outlet of the microchannel, respectively. In the above equation, the second term on the right side represents the pressure drop due to fluid acceleration. Equation 3 reduces to Eq. 2 for the case of incompressible flows. The Poiseuille number is defined as the product of the Darcy friction factor and the Reynolds number:

$$Po = fRe \quad (4)$$

For the case of nitrogen flow in the microchannel, rarefaction effects also become important, specifically for lower mass flow rates. The Knudsen number (Kn) is based on mean hydraulic diameter (D_h) and mean pressure (P_m) and is defined as

$$Kn = \frac{\lambda}{D_h} = \frac{\mu\sqrt{\frac{\pi RT}{2}}}{P_m D_h} \quad (5)$$

where λ is the mean free path of the gas. The maximum uncertainty in Poiseuille number, Reynolds number and Knudsen number is ± 5, ± 4 and ± 0.5%, respectively.

4 Effect of converging/diverging angle on static pressure drop

Figure 4a, b shows the comparison of static pressure drop across the converging (filled symbols) and diverging microchannels (empty symbols) for the case of water and nitrogen, respectively. For both the cases, the pressure drop in converging orientation of the microchannel is higher than that in diverging orientation. This difference is pressure drop of the microchannel when it is subjected to converging and diverging orientation is discussed later in detail in Sect. 7.

In all the cases the pressure drop across the microchannels decreases with increase in diverging/converging angles. In the case of diverging microchannel, increase in the divergence angle decelerates the flow, leading to a larger pressure recovery. Hence, the total pressure drop decreases with increase in the divergence angle. It is intuitively expected that due to greater acceleration at higher convergence angles, the pressure drop should increase with increase in convergence angle. But in the case of the converging microchannels too, the pressure drop is seen to decrease with increasing angle. This is because, although the fluid acceleration is higher for larger convergence angles, the overall pressure drop is dominated by the viscous force rather than the inertial force. This effect of the angles is more clearly understood by studying the force balance in both liquid and gas flows (Sect. 6).

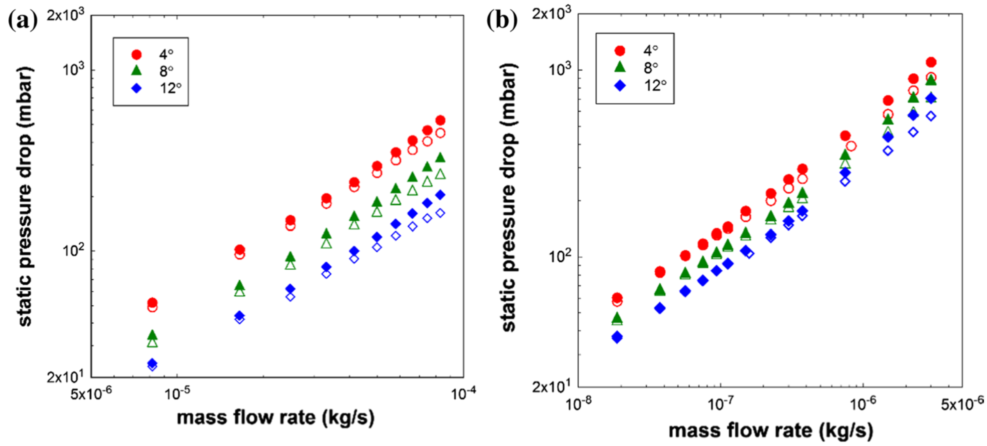

Fig. 4 Static pressure drop variation with mass flow rate for different angles for converging (filled symbols) and diverging microchannels (empty symbols) for **a** water and **b** nitrogen

In some of the earlier studies (Olsson et al. 1996, 2000), instead of pressure drop, the comparison is presented in terms of pressure loss coefficient (ξ) given as

$$\xi = \frac{\Delta P}{\frac{1}{2}\rho v_{\text{throat}}^2} \tag{6}$$

where v_{throat} is the mean velocity of the fluid at the narrowest cross section. In our experiments, to study the effect of diverging/converging angle, the throat area (smallest cross section) is made the same for all the microchannels. Hence, the mean velocity at throat section is the same for all the microchannels, and the ratio of pressure loss coefficients reduces to the ratio of pressure drop across the microchannel, i.e.

$$\frac{\xi_{\text{conv}}}{\xi_{\text{div}}} = \frac{(\Delta p)_{\text{conv}}}{(\Delta p)_{\text{div}}} \tag{7}$$

It should be noted that the end effects are integrated in the measured experimental pressure drop. A similar analysis is carried out by Olsson et al. (2000) and Graur et al. (2014) in the context of gradually diverging/converging microchannels. The end effects of the device are in the form of sudden contraction (or sudden expansion) at the end of the converging/diverging cross section into the reservoir section. These end losses are a function of the area ratio of the entry/exit of the microchannel and the reservoir. The effect of changing the area ratio on the pressure drop due to sudden expansion of the gas at the exit of the microchannel was studied numerically by Hemadri et al. (2017). It was observed that changes in pressure drop characteristics for various reservoir sizes (corresponding to different area ratios) were less than 2%. As our interest is in the utilization of the converging/diverging elements as part of valveless micropumps which include reservoirs (across which the fluid is pumped), the present data provide information on the conditions under which the converging/diverging elements provide maximum pumping efficiency.

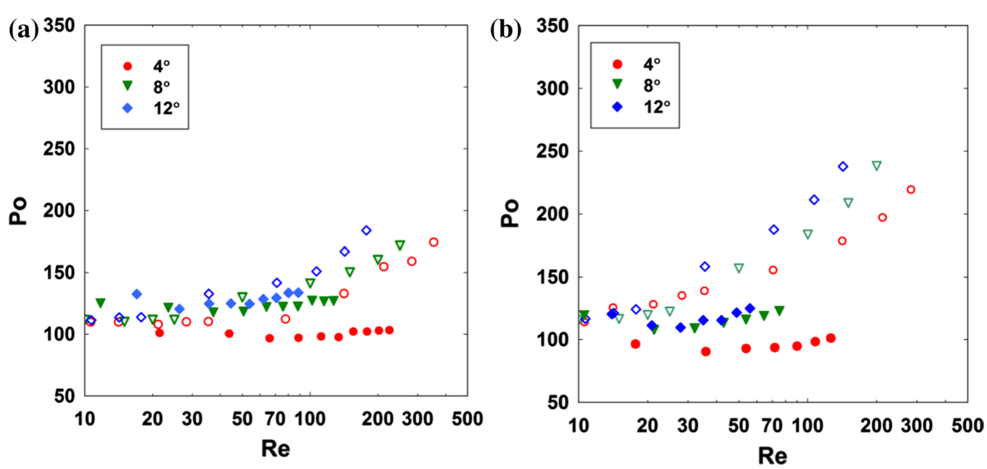

Fig. 5 Variation of Poiseuille number for water (filled symbols) and nitrogen (empty symbols) flow through **a** diverging microchannel, **b** converging microchannel

5 Comparison of Poiseuille number

Figure 5a, b shows the comparison of Poiseuille number for water and nitrogen flowing across diverging and converging microchannels for three different angles. In the case of incompressible, laminar flow, the Poiseuille number is a constant as can be seen from the data corresponding to liquid flow. For the case of gas flows, it is seen that, at lower Reynolds number (*Re* < 50), *Po* is a constant and about 12% higher than the liquid flow. The increase in *Po* for gases in contrast to liquids is attributed to the effect of compressibility of the gas. For *Re* > 50 there is a clear change in slope of *Po* for the case of gas flows. This change of slope corresponds to the case where the maximum Mach number in the flow increases from subsonic velocities (*Ma* < 0.8) to transonic velocities (*Ma* > 0.8). The high Mach numbers lead to high gradients at the throat (narrowest cross section) of the varying cross section microchannel and higher pressure drop due to acceleration caused due to the density variation. The increase in *Po* is more significant in the case of converging microchannels as compared to the diverging orientation of the microchannels because in converging microchannels, apart from the density variation, additional fluid acceleration is caused by the reduction in cross-sectional area.

For very low values of *Re* (< 1), the Knudsen number effect becomes significant for gas flows, and the *Po* starts reducing. Thus, while compressibility effects result in the increase in the *Po*, rarefaction effects act in the opposite sense by decreasing the *Po*. A detailed discussion on the effect of *Kn* on *Po* has already been presented in Hemadri et al. (2017). In both liquid and gas flows, the increase in convergence/divergence angles leads to an increase in the *Po*.

6 Comparison of forces for liquid and gas flows

Figure 6 shows the variation of area-weighted pressure force, inertia force and viscous force along the axis of the 12° diverging and converging microchannel for *Re* = 40 for the case of water and nitrogen. A comparison of the forces in converging microchannel (Fig. 6a, b) shows that the three forces vary similarly along the length of the microchannel for both liquid and rarefied gas flows. Initially, the pressure force is completely balanced by the viscous forces, and the inertial force is negligible. At the exit of the microchannel, there is a large acceleration of

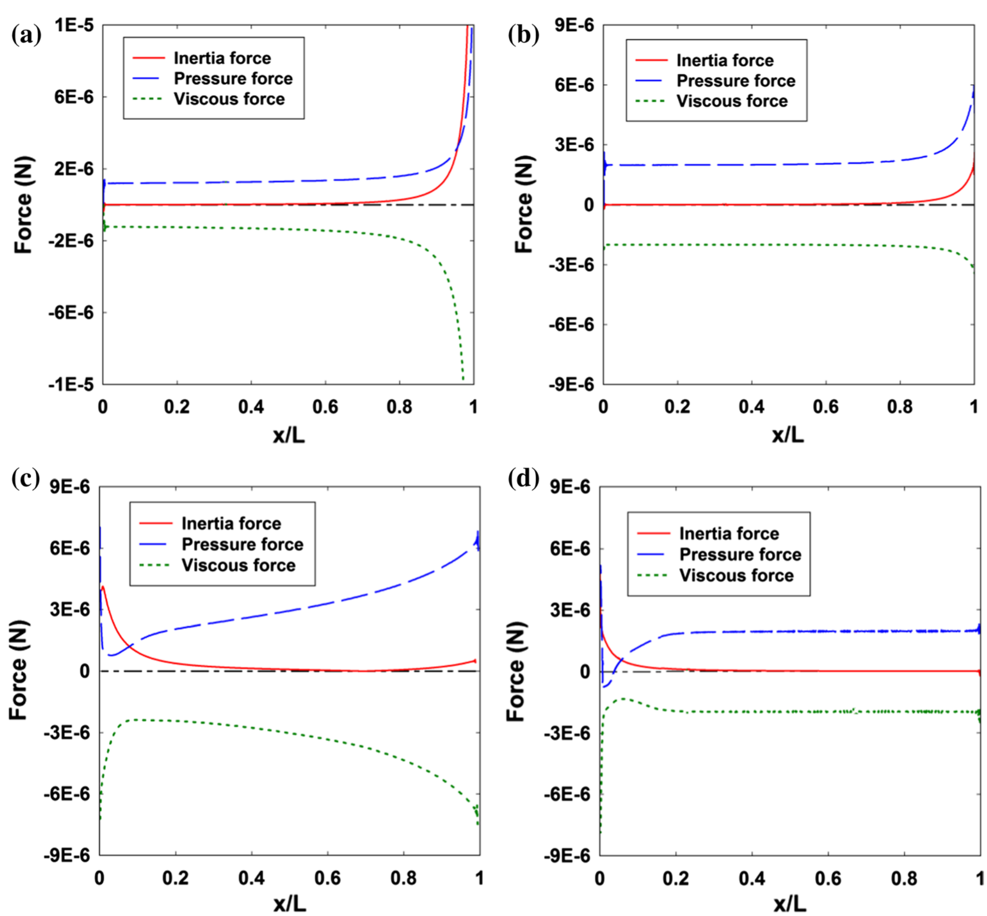

Fig. 6 Streamwise variation of forces in converging microchannel of 12° angle **a** nitrogen, **b** water; and diverging microchannel, **c** nitrogen, **d** water

the fluid resulting in an increase in the inertial force. It is seen that this increase is higher in the case of gas flows which is attributed to the higher acceleration of the gas due to compressibility effects. In the diverging orientation of the microchannel (Fig. 6c, d), the forces in the rarefied gas flow behave quite differently from that of liquid flow. In case of gas flow, there is large pressure recovery along the length of the microchannel, leading to an increase in the pressure force which is balanced by the viscous force. In all the cases, the viscous force is larger than inertial force and the difference is balanced by the pressure force. This is the reason for the increase in pressure drop across the microchannel with decreasing angle, in both converging and diverging orientations.

Another important difference is the presence of a negative gradient at the entrance of the diverging microchannel for the case of water flow. This negative pressure gradient is caused due to the vena contracta effect when the water is made to pass through the throat of the microchannel. Such an adverse pressure gradient is noticeably absent in the case of gas flows, leading to a positive pressure gradient all along the microchannel. This absence of flow reversal is a characteristic of rarefied gas flows and has also been reported in Agrawal et al. (2005) and Varade et al. (2014, 2015b). The existence of slip velocity, momentum diffusivity and negligible kinetic energy together contribute to the absence of flow separation. In microsystems, the kinetic energy is very small compared to the driving pressure energy of the flow. Hence, any change in the kinetic energy does not sufficiently influence the flow to give rise to negative pressure gradient. The higher momentum diffusivity in the case of rarefied gas flows also contributes in the prevention of separation by allowing the gas molecules to diffuse and thus closely follow the microchannel surface.

An entropy generation analysis performed on the 12° converging microchannel gave a peak in entropy generation at the narrowest cross section, which is in line with physical reasoning (the velocity is maximum at the narrowest cross section) and force balance analysis presented here.

7 Diodicity

Fluidic diodicity (D) is the asymmetric transfer in flow passages/devices, which offer a lower flow resistance in one direction and greater resistance in the opposite direction. Diodicity is defined as the ratio for diverging to converging microchannel of the mass flow rate to the difference of square of inlet and outlet pressures. It is given as

$$D = \frac{\dot{m}^{\mathrm{div}} \Big/ \left[\left(P_{\mathrm{i}}^{\mathrm{div}}\right)^2 - \left(P_{\mathrm{o}}^{\mathrm{div}}\right)^2 \right]}{\dot{m}^{\mathrm{conv}} \Big/ \left[\left(P_{\mathrm{i}}^{\mathrm{conv}}\right)^2 - \left(P_{\mathrm{o}}^{\mathrm{conv}}\right)^2 \right]} \tag{8}$$

In the present set of experiments, the mass flow controller is used to obtain the same flow rates in both the converging and diverging orientations. Therefore, Eq. (8) becomes,

$$D = \frac{\left(P_{\mathrm{i}}^{\mathrm{conv}}\right)^2 - \left(P_{\mathrm{o}}^{\mathrm{conv}}\right)^2}{\left(P_{\mathrm{i}}^{\mathrm{div}}\right)^2 - \left(P_{\mathrm{o}}^{\mathrm{div}}\right)^2} = \frac{\left(P_{\mathrm{m}}\Delta P\right)^{\mathrm{conv}}}{\left(P_{\mathrm{m}}\Delta P\right)^{\mathrm{div}}} \tag{9}$$

A diodicity value other than unity implies that there is a flow-directing ability to the microchannel, resulting in different values of pressure drop when the working mode is changed from diverging to converging by reversing the flow direction. For the same mass flow rate, $D > 1$ implies that the pressure drop in the converging mode is higher than that of diverging mode and the reverse is true for $D < 1$.

In the case of liquid flows, few authors (Stemme and Stemme 1993; Olsson et al. 1996, 2000) have studied the diodic effect in converging and diverging orientations of varying cross section microchannel in relation to valveless micropumps. In these studies, it was found that the difference in the mass flow rates across the converging and diverging orientations of the microchannel (for the same inlet and outlet pressures) was due to large pressure recovery and small separation in the diverging mode and gross separation and vena contracta effects in the converging mode of the microchannel.

Figure 7a, b shows the variation of diodicity in the three microchannels of 4°, 8° and 12° for water and nitrogen, respectively. In the case of water, the diodicity approaches unity as the Reynolds number decreases. At higher *Re* (*Re* > 20) the diodicity increases, which corresponds to a higher resistance in the converging mode of the microchannel. As shown by Stemme and Stemme (1993), this greater pressure drop in the converging mode can be attributed to the loss of kinetic energy in the form of a jet at the exit of the microchannel. The rate of increase in diodicity with *Re* is dependent on the angle of convergence/divergence and is higher for higher angles. This is because of larger pressure recovery at higher angles in the case of diverging microchannels. In the case of nitrogen flow in microchannel too, the diodicity is unity for lower Reynolds numbers (*Re* < 10). Similar to the case of water flow, the diodicity increases with increase in *Re*. Here too, the converging orientation has a larger pressure drop, due to the loss of kinetic energy at the exit of the microchannel.

Comparing water and nitrogen values for diodicity shows two important similarities and differences (Fig. 7c). For both fluids, the diodicity value approaches unity as the Reynolds number is lowered. This means that for low *Re* flows, the diodic effect cannot be employed to obtain a pumping action. At higher values of *Re*, for both water and nitrogen, the converging mode has a higher pressure drop, and in this region,

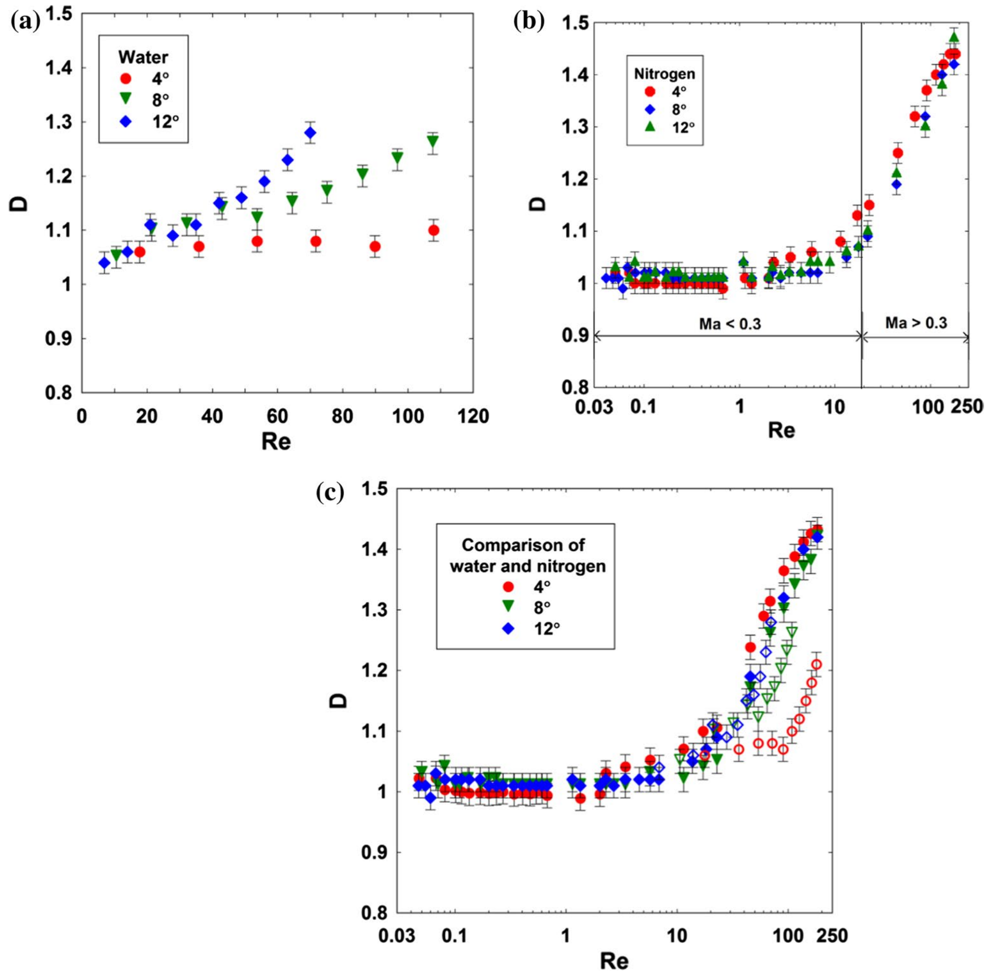

Fig. 7 Diodicity in converging/diverging microchannel as a function of *Re* for **a** water, **b** nitrogen, **c** comparison of water (empty symbols) and nitrogen (filled symbols)

the microchannel has a flow-directing ability which can be used to passively pump the fluid.

The main differences between water and nitrogen are (1) the rise in the value of diodicity is higher in the case of nitrogen, compared to water; (2) unlike water, for nitrogen flow, diodicity is not a strong function of the angle of convergence/divergence. The higher value of diodicity for nitrogen is expected due to the presence of compressibility effects in the case of gas flows. Apart from the acceleration of the gas in the converging microchannel, due to a reduction in the cross-sectional area, there is also an additional acceleration of the gas due to the change in density along the length of the microchannel. In Fig. 7b the data points are divided into two sets based on the outlet Mach number of the flow for converging microchannel. It can be seen that the sudden steep rise in the value of diodicity corresponds to an exit Mach number > 0.3, showing the presence of strong compressibility effects.

In the study performed by Graur et al. (2016), for the case where the varying cross section was obtained by changing the width of the microchannel and the height is kept constant (i.e. $h < w_s$ and $h \ll w_L$; similar to the microchannels

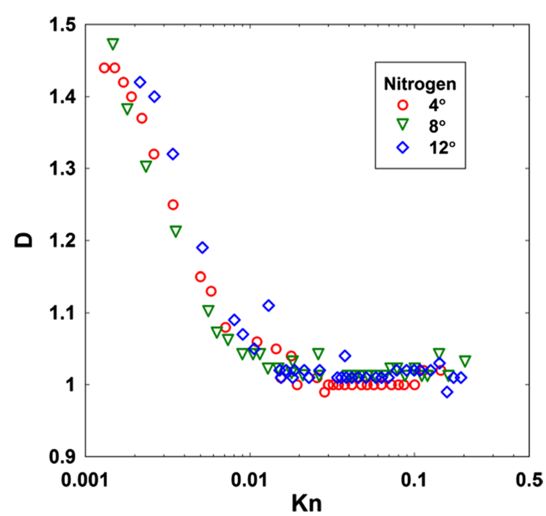

Fig. 8 Effect of Knudsen number on diodicity

employed in the present study), the diodic effect was not observed. When the microchannel height was used as the varying dimension, the diodic effect was seen to exist and to be dependent on the Knudsen number. The data for diodicity as a function of Kn for nitrogen are plotted in Fig. 8 to investigate the effect of gas rarefaction on the diodicity. It is seen that, in the present case, the Knudsen number does not seem to affect the diodicity of the converging/diverging microchannel. If the data points corresponding to compressibility effects ($Ma > 0.3$) are ignored, the diodicity shows a constant value of unity for higher Knudsen numbers ($Kn > 0.01$). The main reason for the absence of Knudsen number effect on diodicity for the present set of microchannels is the negligible influence of the lateral walls on the flow. Due to the considerably higher width compared to the height of the microchannel, the microchannel flow behaves like a flow between parallel plates and the effect of varying width is not noticeable. At higher Re (low Kn), the rarefaction is negligible and compressibility effects dominate the flow leading to the observed diodicity.

8 Design considerations for converging and diverging microchannels

Flow in converging and diverging microchannels has not been studied extensively, and hence, there is lack of theoretical or empirical correlations governing such flows. However, relatively larger data exist for both liquid and gas flows in microchannels of constant cross section. In channels of varying cross sections, the length scale to be employed is not very obvious since the dimensions of the microchannels vary with length. In this regard, it would be advantageous from a designer's perspective, if some sort of a length scale can be proposed for varying cross section microchannels, such that the expressions/correlations that are readily available for constant cross section microchannels can be extended to converging/diverging microchannels. In the present set of experiments, this length scale is called as the 'equivalent hydraulic diameter' and is defined as the hydraulic diameter at an appropriate location along the length of the converging/diverging microchannel (L_{eq} = distance from the narrower end) that gives the same pressure drop as that of a constant cross section microchannel, under identical boundary conditions (Fig. 9).

The algorithm developed to arrive at the equivalent hydraulic diameter for converging and diverging microchannels is similar for both liquid and gas flows. It involves iteratively obtaining the Poiseuille number at different axial locations of the converging/diverging microchannel and comparing it with that obtained by correlations available in the literature for microchannels of constant cross section. A detailed description can be found in Duryodhan et al. (2012, 2014) (liquid flow) and Varade et al. (2015a, b) (gas flow). This section consolidates the results obtained in the above studies and highlights the similarities and differences in the case of water and nitrogen flows.

The value of equivalent hydraulic diameter can be calculated by knowing the width at characteristic location. Generalized form of characteristic width can be represented by

$$w_c = w_s + 2\frac{L}{n}\tan\left(\frac{\theta}{2}\right) \tag{10}$$

where w_c is the width at the characteristic location. Further, n is the divisor whose value varies from 3 to 12.5 based on the mode of operation (i.e. diverging or converging), fluid (i.e. water or nitrogen) and the value of Kn as shown in Table 2.

Table 2 shows that for liquid flows, the concept of equivalent hydraulic diameter is indeed helpful, as its location is seen to be independent of the converging/diverging angle

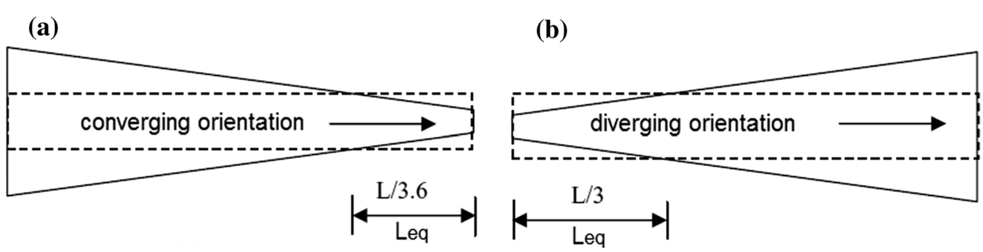

Fig. 9 Schematic showing the location of equivalent hydraulic diameter for water flow in **a** converging microchannel, **b** diverging microchannel

Table 2 Comparison of location of equivalent hydraulic diameter for water and nitrogen

Fluid	Orientation of channel	Location of equivalent hydraulic diameter $L_{eq} = L/n$	Remarks
Water	Converging	$n = 3.6$	Independent of angle and Re
	Diverging	$n = 3$	
Nitrogen	Converging	$n = 3.5–12.5$	Independent of angle and Re, depends on Kn ($0.004 < Kn < 0.1$)
	Diverging	$n = 3.5–12.5$	

L_{eq} should be measured from the narrower end of microchannel and the Reynolds number. It should also be noted that the L_{eq} for converging microchannel is smaller than its diverging counterpart, indicating that the pressure drop in the converging orientation is higher than the diverging orientation. This difference in the pressure drop across the microchannel when subjected to converging/diverging orientation is due to the diodic effect discussed in the previous section.

For the case of nitrogen, since the flow is rarefied, the Knudsen number comes into the picture and hence the location for equivalent hydraulic diameter is no longer unique but depends on the amount of rarefaction. Nevertheless, the concept of equivalent hydraulic diameter will facilitate to extend the use of available correlations made for uniform cross section microchannels to that of diverging/converging microchannels. Furthermore, it is useful to derive the theoretical formulae to calculate engineering numbers in terms of geometrical parameters at characteristic location.

As seen from Table 2, as Knudsen number increases, L_{eq} gets smaller. With further increase in rarefaction the equivalent hydraulic diameter corresponds to the smallest cross-sectional area. It is therefore appropriate to calculate the flow parameters at the smallest cross section while designing the converging/diverging microchannel to operate at higher rarefaction ($Kn > 0.1$).

9 Conclusions

In this paper, the comparison between converging and diverging orientations of varying cross section microchannels was presented for liquid and gas flows. The effect of converging/diverging angle on the static pressure drop is studied, and it is seen that the pressure drop increases with decreasing converging/diverging angle for both liquid and gas flows. The effect of fluid on the Poiseuille number is presented. It is seen that the *Po* is a constant for the case of liquid flows, whereas in the case of gas flows, *Po* is seen to be affected by compressibility and rarefaction effects. The various forces along the microchannel for liquid and gas flows are discussed. The force comparison shows a large pressure recovery in gas flow in diverging microchannels in contrast to liquid flows. The absence of flow reversal is another important characteristic of rarefied gas flow in microchannels.

The effect of Reynolds number, Mach number and Knudsen number on the existence of diodicity is investigated. It is seen that for lower Reynolds numbers the diodic effect is absent in the case of both liquid and gas flows. Hence, the range of operation of converging/diverging elements as flow-directing valves in a micropump will be restricted by the Reynolds number. The concept of equivalent hydraulic diameter is presented which facilitates the use of correlations of constant cross section microchannels to predict the flow properties in converging/diverging microchannels. It is seen that such a diameter is more relevant to the case of liquid flows (where it is independent of flow and geometric properties) as compared to slightly rarefied gas flows (where the location of equivalent hydraulic diameter is seen to depend on Knudsen number). However, at higher rarefactions ($Kn > 0.1$), the equivalent hydraulic diameter converges to the smallest cross-sectional area of the microchannel and hence the flow parameters obtained at this location should be utilized to design converging/diverging microchannels.

Acknowledgements We are grateful to the Department of Science and Technology, New Delhi, for funding this study.

References

Agrawal A, Djenidi L, Antonia RA (2005) Simulation of gas flow in microchannels with a sudden expansion or contraction. J Fluid Mech 530:135–144

Agrawal A, Duryodhan VS, Singh SG (2012) Pressure drop measurements with boiling in diverging microchannel. Front Heat Mass Transf 3:013005

Akbari M, Sinton D, Bahrami M (2010) Laminar fully developed flow in periodically converging-diverging microtubes. Heat Transf Eng 31(8):628–634

Akbari M, Sinton D, Bahrami M (2011) Viscous flow in variable cross-section microchannels of arbitrary shapes. Int J Heat Mass Transf 54:3970–3978

Duryodhan VS, Singh SG, Agrawal A (2012) Liquid flow through a diverging microchannel. Microfluid Nanofluid 14:53–67

Duryodhan VS, Singh SG, Agrawal A (2014) Liquid flow through a converging microchannel and comparison with diverging microchannel. J Micromech Microeng 24:125002

Gerlach T (1998) Microdiffusers as dynamic passive valves for micropump applications. Sens Actuators A 69:181–191

Graur I, Veltzke T, Meolans JG, Ho MT, Thöming J (2014) The gas flow diode effect: theoretical and experimental analysis of moderately rarefied gas flows through a microchannel with varying cross section. Microfluid Nanofluid 18(3):391–402

Graur I, Méolans JG, Perrier P, Thöming J, Veltzke T (2016) A physical explanation of the gas flow diode effect. Microfluid Nanofluid 20:145

He X, Zhu J, Zhang X, Xu L, Yang S (2017) The analysis of internal transient flow and the performance of valveless piezoelectric micropumps with planar diffuser/nozzles elements. Microsyst Technol 23:23–37

Hemadri V, Varade VV, Agrawal A, Bhandarkar UV (2016) Investigation of rarefied gas flow in microchannels of non-uniform cross section. Phys Fluids 28(2):022007

Hemadri V, Varade VV, Agrawal A, Bhandarkar UV (2017) Rarefied gas flow in converging microchannel in slip and early transition regimes. Phys Fluids 29:032002

Lauga E, Stroock AD, Stone HA (2004) Three-dimensional flows in slowly varying planar geometries. Phys Fluids 16:3051–3062

Olsson A, Stemme E, Stemme G (1996) Diffuser element design investigation for valve-less pumps. Sens Actuators A 57:137–143

Olsson A, Stemme E, Stemme G (2000) Numerical and experimental studies of flat-walled diffuser elements for valve-less micropumps. Sens Actuators 84:165–175

Sharipov F, Bertoldo G (2005) Rarefied gas flow through a long tube of variable radius. J Vac Sci Technol A 23(3):531–533

Singh SG, Kulkarni A, Duttagupta SP, Puranik BP, Agrawal A (2008) Impact of aspect ratio on flow boiling of water in rectangular microchannels. Exp Thermal Fluid Sci 33:153–160

Singhal V, Garimella SV, Murthy JY (2004) Low Reynolds number flow through nozzle–diffuser elements in valveless micropumps. Sens Actuators A 113:226–235

Stemme E, Stemme G (1993) A valveless diffuser/nozzle-based fluid pump. Sens Actuators A39:159–167

Szalmas L, Veltzke T, Thöming J (2015) Analysis of the diodic effect of flows of rarefied gases in tapered rectangular channels. Vacuum 120:147–154

Tanaka S, Miyazaki K, Fujiwara S (2013) Pump head improvement of diffuser/nozzle valve-less micropump. In: Proceedings of the ASME 11th international conference on nanochanels, microchannels and minichannels

Varade V, Agrawal A, Pradeep AM (2014) Behaviour of rarefied gas flow near the junction of a suddenly expanding tube. J Fluid Mech 739:363–391

Varade V, Duryodhan VS, Agrawal A, Pradeep AM, Ebrahimi A, Roohi E (2015a) Low Mach number slip flow through diverging microchannel. Comput Fluids 111:46–61

Varade V, Agrawal A, Pradeep AM (2015b) Slip flow through converging microchannel: experiments and three-dimensional simulations. J Micromech Microeng 25:025015